Signal Processing 29 (1992) 265–281
Elsevier

Estimation of optimal morphological τ-opening parameters based on independent observation of signal and noise pattern spectra

Edward R. Dougherty
Center for Imaging Science, Rochester Institute of Technology, Rochester, NY 14623, USA

Robert M. Haralick
Department of Electrical Engineering, University of Washington, Seattle, WA 98195, USA

Yidong Chen
Center for Imaging Science, Rochester Institute of Technology, Rochester, NY 14623, USA

Carsten Agerskov, Ulrik Jacobi and Poul Henrik Sloth
Department of Electrical Engineering, Technical University of Denmark, 2800 Lyngby, Denmark

Received 3 February 1992

Abstract. A classical morphological technique to restore binary images degraded by union noise is to perform an opening to remove the noise. The more general approach is to employ a union of openings, the resulting filter being known as a τ-opening. Assuming the structuring elements to be parameterized in terms of a single parameter, a fundamental problem is to determine the optimal parameter, namely the one that produces the filter having minimum error according to some error measure. Relative to symmetric-difference error and a certain random-grain model, the present paper develops an optimization procedure based upon the individual pattern spectra of the signal and noise. If the image and noise grains are disjoint, then the pattern-spectra parametric estimation procedure yields exactly the optimal value of the parameter. Of special concern in the present paper is the robustness of the method with respect to the disjointness criterion. It is analytically demonstrated for a particular model that the estimation procedure produces close to the optimal value when image and noise are not disjoint. Robustness is also experimentally demonstrated for a large number of more complex image-noise models.

Zussammenfassung. Eine klassische Methode zur Restaurierung von bildern, die durch Rauschen gestört sind, besteht in der Anwendung eines 'Openings' zur Entfernung des Rauschens. Eine verallgemeinerte Lösung liegt in der Verwendung einer 'Union of Openings'; das resultierende Filter ist als τ-Opening bekannt. Unter der Annahme, daß die Strukturelemente in Form eines einzelnen Parameters dargestellt sind, ist das fundamentale Problem die Festlegung des optimalen Parameters, nämlich desjenigen, der zu einem Filter mit minimalem Fehler bezüglich einiger Fehlermessungen führt. Im Vergleich zum 'symmetric-difference'-Fehler und einem bestimmten 'random-grain'-Modell wird in der vorliegenden Arbeit eine optimierte Prozedur entwickelt, die auf den individuellen Spektralmustern des Signals und des Rauschens basieren. Wenn sich beide ausschließen, dann liefert die Parametrische Schätzung der Spektralmuster exakt den optimalen Parameterwert. Von besonderem Interesse ist in der vorliegenden Arbeit die Robustheit der Methode in bezug auf das 'disjointness'-Kriterium. Für ein spezielles Modell wird analytisch gezeigt, daß die Schätz-Prozedur nahezu optimale Werte liefert, wenn Bild und Störung sich ausschließen. Die Robustheit wird weiterhin experimentell demonstriert anhand einer großen Anzahl von komplexeren Bild-Störungs-Modellen.

Correspondence to: E.R. Dougherty, Center for Imaging Science, Rochester Institute of Technology, Chester F. Carlson Building, P.O. Box 9887, Rochester, NY 14623-0887, USA.

0165-1684/92/$05.00 © 1992 Elsevier Science Publishers B.V. All rights reserved

Résumé. Une technique morphologique classique pour restaurer des images binaires, dégradées par l'union de bruit, consiste à réaliser une ouverture pour éliminer le bruit. Une approche plus générale consiste à utiliser une union d'ouverture, le filtre résultant étant connu comme l'ouverture τ. En admettant que les éléments structurants n'ont qu'un seul paramètre, un problème fondamental consiste à dèterminer la valeur optimale du paramètre, c'est-à-dire celle qui produit le filtre ayant l'erreur minimum selon une mesure donnée. Cet article développe une procédure d'optimisation basée sur le spectre des formes individuelles du signal et du bruit, relative à l'erreur de différence symétrique et à un cetain modèle de grains aléatoires. Si l'image et les grains de bruit sont disjoints, alors la procédure d'estimation paramétrique du spectre de la forme donne exactement la valeur optimale du paramètre. La robustesse de la méthode, par rapport au critère d'être disjoint, est un sujet qui est traité avec une attention particulière. Il est démontré analytiquement, pour un modèle particulier, que la procédure d'estimation produit une valeur proche de celle qui est optimale quand l'image et le bruit ne sont pas disjoints. La robustesse est également démontrée expérimentalement pour un grand nombre de modèles complexes d'images et de bruit.

Keywords. Mathematical morphology; optimal filtering; pattern spectrum; granulometry; τ-opening; union noise.

1. Introduction

A classical problem in binary morphological filtering involves the restoration of an image that has been corrupted by union noise. Specifically, S is the desired signal, N is the noise, and $S \cup N$ is observed. A well-known approach to this problem, due to Matheron [15], involves the use of τ-opening filters. In the present paper we develop a methodology to select an optimal τ-opening from among a class of τ-openings. The method involves application of Matheron's granulometric method to both signal and noise, the resulting size distributions being popularly known as the pattern spectra of the signal and noise.

To appreciate the genesis of the method, consider the ordinary *morphological opening* $O(S, E)$ of the image S by the structuring element E, defined by $O(S, E) = \bigcup \{E+x : E+x < S\}$, where $E+x$ is the translation of E by x, namely $E+x = \{e+x : e \in E\}$ and $<$ denotes the subset relation. A point z lies in the opening $O(S, E)$ if and only if there exists some translate $E+x$ such that $z \in E+x < S$. As a filter, opening by E passes those portions of S that match some translate of E and filters out the remainder of S. If we now consider a corrupted image $S \cup N$, where S is the uncorrupted image and N is noise, then the object is to find a structuring element that passes most of S and very little of N. If we assume that S and N are compact and disjoint, and that E fits into all of the connected components of S but not into any of the connected components of N, then N will be completely eliminated and all of S that conforms to the shape and size of E will remain. Typically, however, even if the signal and noise components are disjoint, there will be size overlap, meaning that some large components of N will be greater than some small components of S. This situation is analogous to linear-space filtering when the Fourier representations of signal and noise share basis components. The goal is to achieve optimality when the sizes of signal and noise components intermingle.

Our approach is to model the signal and noise as random Boolean images whose components are known shapes, possessing random sizing parameters, that are randomly tossed into the plane. Note that disjointness of the components actually places a constraint on full randomness (as would be the case with Poisson points). Our goal is to find optimal-sized structuring elements by which to filter the corrupted signal under the assumption that we know the morphological pattern spectra of the signal and noise, but not of the corrupted signal. In effect, we have some independent morphological knowledge of the signal and the corrupting noise. Such a situation would occur if we had a thresholded image composed of desirable and undesirable particles, and we had knowledge of both particle processes. It would also occur if we wished to remove background objects of noninterest from foreground objects of interest. (More will be said on such modeling following the theory and the simulations.) Having solved the problem in full for disjoint signal and noise, we proceed to demonstrate, in part theoretically and in part through simulation, the degree to which the estimation procedure in the disjoint case can be applied to the

case of nondisjoint signal and noise. The key point is: while there is some loss of accuracy in applying the procedure when the disjointness criterion does not hold, this loss is minimal should signal–noise overlap not be too great. In fact, such is often the case: just think of touching grains or touching texture primitives.

2. Granulometric pattern spectra

We begin by briefly reviewing the Matheron granulometric theory. Binary morphological τ-openings compose an important class of morphological filters. According to Matheron, a binary filter Ψ is a *τ-opening* if it satisfies four conditions: Ψ is *increasing*: $S<T$ implies $\Psi(S)<\Psi(T)$; Ψ is *antiextensive*: $\Psi(S)<S$; Ψ is *translation invariant*: $\Psi(S+x)=\Psi(S)+x$; Ψ is *idempotent*: $\Psi[\Psi(S)]=\Psi(S)$. The most commonly employed τ-opening is the ordinary opening.

A key aspect of any filter is its *invariant* class, which consists of those images that are preserved under the filter. We will denote the invariant class of a τ-opening Ψ by $\mathrm{Inv}[\Psi]$, so that $S\in\mathrm{Inv}[\Psi]$ if and only if $\Psi(S)=S$. Since Ψ is idempotent, $\Psi(S)\in\mathrm{Inv}[\Psi]$ for any S. If $\boldsymbol{B}$ is a collection of images such that each image in $\mathrm{Inv}[\Psi]$ is a union of translates of elements in $\boldsymbol{B}$, then $\boldsymbol{B}$ is called a *base* for Ψ. Intuitively, $\boldsymbol{B}$ consists of image primitives that generate the invariants of Ψ. As shown by Matheron [15], Ψ is a binary τ-opening if and only if there exists a class $\boldsymbol{B}$ of images such that $\Psi(S)=\bigcup\{O(S,B): B\in\boldsymbol{B}\}$. Moreover, $\boldsymbol{B}$ is a base for Ψ; in fact, any base will do. It is immediate that a τ-opening is determined by any base. Consequently, optimization of τ-opening filters means finding an optimal base, where perhaps the optimization is constrained to some class of potential bases.

Closely related to τ-openings are granulometries, which were conceived by Matheron as a model for sieving within an image. (For a full description of binary τ-openings and granulometries see Serra [21] or Dougherty and Giardina [2, 8]). A *granulometry* is a parameterized family of filters Ψ_r, $r>0$, such that Ψ_r is increasing, Ψ_r is antiextensive, and $\Psi_r\Psi_s=\Psi_s\Psi_r=\Psi_{\max\{r,s\}}$. To complete the definition of a granulometry we let $\Psi_0(S)$ be the identity mapping. The granulometry is denoted by $\{\Psi_r\}$. If $r\geq s>0$, then $\mathrm{Inv}[\Psi_r]<\mathrm{Inv}[\Psi_s]$. A *$\tau$-granulometry* is a granulometry $\{\Psi_r\}$ for which Ψ_r is translation invariant. The most commonly employed τ-granulometries are the elementary granulometries, each of these being of the form $\Psi_r(S)=O(S,rB)$, where B is a convex primitive.

For application, a key property of any granulometry $\{\Psi_r\}$ is that, for $r\geq s$, $\Psi_r(S)<\Psi_s(S)$. Thus, if $A[S]$ denotes image area (and S possesses finite area), then $\{A[\Psi_r(S)]\}$ is decreasing. If we define $\Phi(r)=1-A[\Psi_r(S)]/A[S]$, then $\Phi(0)=0$, $\Phi(r)$ is increasing, and the limit of $\Phi(r)$ as $r\to+\infty$ is 1. Under conditions that typically hold in application, it can be shown that $\Phi(r)$ is continuous from the left, so that $\Phi(r)$ is a probability distribution function (PDF) and its derivative $\mathrm{d}\Phi(r)$ is a probability density. (In the digital case the continuity condition is inapplicable, so that $\Phi(r)$ is a discrete PDF and $\mathrm{d}\Phi(r)$ is a probability mass function.) Φ and $\mathrm{d}\Phi$ have historically been called *size distributions*, a terminology in line with their granulometric derivation; however, owing to their shape discrimination capability, they have more recently been called *pattern spectra*. Typically, the moments of $\mathrm{d}\Phi$ are employed for image analysis. For instance, Maragos [12–14] has considered shape analysis and symbolic image modeling, Serra [21] has employed size distributions for both shape and texture analysis, and Dougherty et al. [4–7, 16] have used size distributions for analysis, segmentation and classification based upon texture.

Recently, Agerskov et al. [1] have considered the problem of estimating morphological-filter parameters for restoration in the $S\cup N$ noise model. Generically, one can consider a parameterized filter class $\{\Psi_r\}$, not necessarily a granulometry, and attempt to find some rule for estimating a good value of r by considering the signal and noise processes. In [1], it is assumed that the signal and noise

pattern spectra (or generalized versions thereof) are known, and based upon these spectra one wishes to estimate an optimal value of r. The procedure employed is to try to find some multiple linear regression of r on parameters derived from the pattern spectra. Of the four filters considered, two are τ-openings. Although in some cases in [1] the estimations are reasonably good, the evident difficulty with the approach is use of linear regression without an underlying model to justify supposition of the multi-linear model. Nonetheless, in the case of τ-openings, their close relation to granulometries points to the plausibility of a pattern-spectra based estimation procedure. It is the purpose of this paper to explore just such an approach in the case of a certain grain model.

3. Filtering in the deterministic disjoint model

Consider a parameterized collection of convex structuring-element primitives $B_1(r)$, $B_2(r), \ldots,$ $B_m(r)$ such that for $k=1, 2, \ldots, m$, and for $r \geqslant s$, $O[B_k(r), B_k(s)] = B_k(r)$. For any image F, define

$$\Psi_r(F) = O(F, B_1(r)) \cup O(F, B_2(r)) \cup \cdots \cup O(F, B_m(r)). \tag{1}$$

Then $\{\Psi_r\}$ is τ-granulometry, Ψ_r is a τ-opening for any r, and relative to $\{\Psi_r\}$, the signal S and the noise N possess pattern spectra given by

$$\begin{aligned} \Phi_S(r) &= 1 - A[\Psi_r(S)]/A[S], \\ \Phi_N(r) &= 1 - A[\Psi_r(N)]/A[N]. \end{aligned} \tag{2}$$

For fixed r, we can treat $S^\wedge = \Psi_r(S \cup N)$ as an estimator of S, keeping in mind that $S^\wedge$ depends on r. By the increasing monotonicity and antiextensivity of Ψ_r, $\Psi_r(S) < S^\wedge < S \cup N$. If it happens that S is invariant under Ψ_r (an assumption we do not wish in general to make), then the preceding inequality becomes $S < S^\wedge < S \cup N$. Unless S is Ψ_r-invariant, it is possible (and likely) that $S^\wedge$ will not contain S. In any event, our goal is to find the value of r that minimizes the symmetric-difference error

$$e(r) = A[(S - S^\wedge) \cup (S^\wedge - S)]. \tag{3}$$

Let us now make the assumption that S and N are disjoint. Though this assumption is only realistic for sufficiently sparse S and sufficiently sparse N, it leads to a very tractable model, one which provides essential insight. For this model,

$$e(r) = A[N](1 - \Phi_N(r)) + A[S]\Phi_S(r). \tag{4}$$

The optimal value of r is found by minimizing this sum over r. If we assume that Φ_N and Φ_S are differentiable, then taking the derivative with respect to r and setting $e'(r)$ equal to zero yields $A[N]\,\mathrm{d}\Phi_N(r) = A[S]\,\mathrm{d}\Phi_S(r)$. Although this last equation is attractive and perhaps useful for some general insight, (4) is more important because we will be dealing with delta-function derivatives. Moreover, in a digital implementation, minimization of (4) involves finding $e(r)$ for a finite set of values and then selecting the minimum. Examination of (4) shows that

$$e(r) = e_N(r) + e_S(r), \tag{5}$$

where $e_N(r)$ is the error resulting from noise not eliminated by Ψ_r and $e_S(r)$ is the error resulting from erroneously eliminated signal. It is this decomposition of the error that yields straightforward optimization in the disjoint model.

4. The case of a single convex base image

To obtain an analytical solution, we consider the simple case of a single opening by rB, where B is convex. In addition, we assume

$$\begin{aligned} S &= s_1 B + x_1 \cup s_2 B + x_2 \cup \cdots \cup s_a B + x_a, \\ N &= n_1 B + y_1 \cup n_2 B + y_2 \cup \cdots \cup n_b B + y_b, \end{aligned} \tag{6}$$

where $s_i \leqslant s_{i+1}$, $n_i \leqslant n_{i+1}$, the convex components $s_i B + x_i$ are mutually disjoint, and so too are the

components n_iB+y_i. Thus, the noise image is

$$S\cup N=(s_1B+x_1\cup\cdots\cup s_aB+x_a)\cup(n_1B+y_1\cup\cdots\cup n_bB+y_b). \quad (7)$$

The signal and the noise areas are

$$A[S]=(s_1^2+s_2^2+\cdots+s_a^2)A[B],\qquad A[N]=(n_1^2+n_2^2+\cdots+n_b^2)A[B]. \quad (8)$$

Owing to disjointness, $A[S\cup N]=A[S]+A[N]$. In differential form, the signal and noise pattern spectra are

$$\mathrm{d}\Phi_S=A[S]^{-1}A[B](s_1^2\delta(r-s_1)+s_2^2\delta(r-s_2)+\cdots+s_a^2\delta(r-s_a)),$$
$$\mathrm{d}\Phi_N=A[N]^{-1}A[B](n_1^2\delta(r-n_1)+n_2^2\delta(r-n_2)+\cdots+n_b^2\delta(r-n_b)). \quad (9)$$

For $r\geqslant 0$, let $a(r)$ denote the greatest index s_i such that $s_i<r$ and $b(r)$ denote the greatest index n_i such that $n_i<r$. Then

$$\Phi_S(r)=A[S]^{-1}A[B](s_1^2+s_2^2+\cdots+s_{a(r)}^2),\qquad \Phi_N(r)=A[N]^{-1}A[B](n_1^2+n_2^2+\cdots+n_{b(r)}^2). \quad (10)$$

Hence, (4) becomes

$$\begin{aligned}e(r)&=A[N]-A[B](n_1^2+n_2^2+\cdots+n_{b(r)}^2)+A[B](s_1^2+s_2^2+\cdots+s_{a(r)}^2)\\&=A[B](s_1^2+s_2^2+\cdots+s_{a(r)}^2)+A[B](n_{b(r)+1}^2+n_{b(r)+2}^2+\cdots+n_b^2),\end{aligned} \quad (11)$$

where the first summand is $e_S(r)$ and the second is $e_N(r)$.

For given deterministic images S and N, the best opening filter $O(S\cup N, rB)$ is found by minimizing $e(r)$ in (11). As is typically the case, statistical optimization requires extension to random images and random noise.

5. Statistical optimization

Turning to the nondeterministic setting, we first consider the simple model in which S is a union of sB components, where now each value of s is selected from a known probability distribution (random variable) $\boldsymbol{S}$ possessing density $f_S(s)$. We also assume N is a union of nB components, each value of n arising from a known probability distribution $\boldsymbol{N}$ possessing density $f_N(n)$. Let us also assume that the mean of $\boldsymbol{N}$ is less than the mean of $\boldsymbol{S}$, i.e., $\mathrm{E}[\boldsymbol{N}]<\mathrm{E}[\boldsymbol{S}]$. This will assure us of some ability to filter out the noise by rB components (for suitable values of r). Finally, let us assume that the signal possesses a components and the noise possesses b components. Although a and b could be random, for the purpose of obtaining a closed-form solution, let us avoid this complication. Under the assumptions, both S and N are random images and realizations of S and N take the forms given by (6).

In the extreme case, there exists r_0 such that $\boldsymbol{N}<r_0<\boldsymbol{S}$, so that the maximum size of the noise components must be less than the minimum size of the signal components. For r_0, both summands in (11) are vacuous, so that $e(r_0)=0$ for any realization of the observation $S\cup N$. Consequently, opening by r_0B is optimal and there is perfect restoration.

More generally, since S, N and $S\cup N$ are random images, Φ_S, Φ_N, $\mathrm{d}\Phi_S$ and $\mathrm{d}\Phi_N$ are random signals. Moreover, the error $e(r)$ is a random function of r. This is true in both the general disjoint model, Eq. (4), as well as in the specific model involving a single generating primitive B. Thus, our real estimation problem involves finding r to minimize $E[e(r)]$, the expected-value function for $e(r)$. Letting $r^\wedge$ denote this minimum, in the general τ-opening model our optimal filter is $\Psi_{r^\wedge}(S\cup N)$, and, in the single-opening model of (11), the optimal filter is $O(S\cup N, r^\wedge B)$.

Referring to (6), let us find an expression for $E[e(r)]$. Let $\boldsymbol{Y}=\boldsymbol{S}^2$ for $\boldsymbol{S}<r$ and $\boldsymbol{Y}=0$ for $\boldsymbol{S}\geqslant r$. Then in the random model, $e_S(r)=A[B](\boldsymbol{Y}_1+\boldsymbol{Y}_2+\cdots+\boldsymbol{Y}_a)$, where $\boldsymbol{Y}_i$ is identically distributed to $\boldsymbol{Y}$ for $i=1,2,\ldots,a$. Similarly, if $\boldsymbol{Z}=\boldsymbol{N}^2$ for $\boldsymbol{N}\geqslant r$, and $\boldsymbol{Z}=0$ for $\boldsymbol{N}<r$, then $e_N(r)=A[B](\boldsymbol{Z}_1+\boldsymbol{Z}_2+\cdots+\boldsymbol{Z}_b)$, where $\boldsymbol{Z}_i$ is identically distributed to $\boldsymbol{Z}$ for $i=1,2,\ldots,b$. Taking

expected values yields

$$\mathrm{E}[e_S(r)] = bA[B]\,\mathrm{E}[\boldsymbol{Y}] = aA[B]\int_0^r s^2 f_S(s)\,\mathrm{d}s,$$
$$\mathrm{E}[e_N(r)] = bA[B]\,\mathrm{E}[\boldsymbol{Z}] = bA[B]\int_r^\infty n^2 f_N(n)\,\mathrm{d}n. \tag{12}$$

The optimal value of r is that which minimizes

$$\mathrm{E}[e(r)] = A[B]\left(a\int_0^r x^2 f_S(x)\,\mathrm{d}x + b\int_r^\infty x^2 f_N(x)\,\mathrm{d}x\right). \tag{13}$$

Minimization of (13) characterizes the optimal opening $O(S \cup N, r\,\hat{}\,B)$. As noted above, if $f_S(s) = 0$ for $s < r_0$ and $f_N(n) = 0$ for $n > r_0$, then r_0 is optimal and $\mathrm{E}[e(r_0)] = 0$.

Whereas appeal to differentiation for optimization is generally not useful in the deterministic setting, it often can be applied in the random setting. Differentiation of (13) with respect to r yields

$$e'(r) = A[B](ar^2 f_S(r) - br^2 f_N(r)). \tag{14}$$

Since the minimizing value of r does not occur at 0, after setting $e'(r) = 0$ we can divide out r to obtain $af_S(r) = bf_N(r)$. Of course, this last equation may not possess a unique solution for r and its solution may not give the optimal value of r; however, in many practical cases, it may be solved for optimal r. If not, then optimization in the discrete case can be acheived by examining a finite collection of $\mathrm{E}[e(r)]$ values.

If we return to the general disjoint model of (4), then $e(r)$ is again a random function of r; however, it is much more complicated, because not only are the differential pattern spectra generally not delta functions, but $A[S]$ and $A[N]$ do not drop out, and these are both random variables depending on the realizations of S and N. In terms of expectation,

$$\mathrm{E}[e(r)] = \mathrm{E}[A[N](1 - \Phi_N(r))] + \mathrm{E}[A[S]\Phi_S(r)]. \tag{15}$$

Note that the noise and signal areas are not statistically independent of their respective spectra, so that no further simplification is possible. In digital implementation, r is discrete and minimization occurs numerically.

Before considering the case for which signal and noise are not disjoint, we would like to mention the morphological restoration work of Schonfeld and Goutsias [17–19], who also make use of the pattern spectrum, although in quite a different vein. They define a smoothness criterion for the filtered image by requiring the pattern spectrum of the filtered image to be null for small spectrum values, thereby determining that the filtered image is invariant for openings by sufficiently small structuring elements (and invariant for closings by sufficiently small structuring elements, since they also employ closing granulometries). They use the smoothness criterion in conjunction with a *least mean difference criterion* to define optimality, the latter criterion employing, as we do, symmetric difference to measure error. Using their dual criteria, they show that, among a certain class of filters, optimal restoration is achieved by employing certain alternating sequential filters (see [20]). The similarities to our approach are use of the pattern spectrum, the symmetric-difference criterion of goodness, and a random-grain noise model; major differences are the image model (which we take to be random-grain and they take to be deterministic), the class of filters over which optimization is taking place, the manner in which pattern spectra are employed, and our determination, under certain conditions, of a closed-form optimization equation [eq. (13)] and its analytic solution.

Perhaps it should also be pointed out that Schonfeld and Goutsias make a second use of the pattern spectrum, albeit one that is somewhat heuristic (but very interesting). Let γ_B denote opening by B, ϕ_B denote closing by B, and kB denote self-dilation of B k times. Consider a parameterized alternating-sequential-filter family defined by $\Psi_k = \phi_{kB}\gamma_{kB}\phi_{(k-1)B}\gamma_{(k-1)B}\cdots\phi_B\gamma_B$, where B is a fixed set. Schonfeld and Goutsias find an expression for the member Ψ_μ of the family that provides optimal restoration for their degradation model. The difficulty is that the parameter μ is an

unknown associated with the degradation process and requires estimation. In the absence of an optimal estimation rule for μ, they employ a plausible heuristic argument to 'derive' a method of 'estimating' μ from the pattern spectrum of the degraded image.

6. Signal and noise not disjoint: analysis of the general problem

For nondisjoint signal and noise, the decomposition of (5) holds once again, the error terms $e_S(r)$ and $e_N(r)$ giving the areas of S_r, the signal erroneously removed by the filter, and N_r, the noise erroneously not removed; however, these areas are not given by the spectra terms of (4). Decomposing the observed image by $S \cup N = S \cup (N-S)$ shows

$$\begin{aligned} S_r &= S - \Psi_r(S \cup N) = S \cap \Psi_r(S \cup N)^c, \\ N_r &= N - \Psi_r(S \cup N)^c = N \cap \Psi_r(S \cup N), \\ e(r) &= A[S - \Psi_r(S \cup N)] + A[N \cap \Psi_r(S \cup N)]. \end{aligned} \tag{16}$$

To treat nondisjoint S and N, let

$$\begin{aligned} d_S(r) &= A[S]\Phi_S(r), \\ d_N(r) &= A[N](1 - \Phi_N(r)), \\ d(r) &= d_S(r) + d_N(r). \end{aligned} \tag{17}$$

In the disjoint signal and noise model, the first two equations of (16) reduce to

$$\begin{aligned} S_r &= S - [\Psi_r(S) \cup \Psi_r(N)] = S - \Psi_r(S), \\ N_r &= N \cap [\Psi_r(S) \cup \Psi_r(N)] = N \cap \Psi_r(N), \end{aligned} \tag{18}$$

so that

$$\begin{aligned} e_S(r) &= A[S] - A[\Psi_r(S)] = d_S(r), \\ e_N(r) &= A[(N \cap \Psi_r(S)) \cup (N \cap \Psi_r(N))] \\ &= A[\Psi_r(N)] = d_N(r), \end{aligned} \tag{19}$$

$e(r) = d(r)$, and (4) holds. But these equalities do not hold in general.

What can be said in general is that $e_S(r) \leqslant d_S(r)$ and $e_N(r) \geqslant d_N(r)$. Both inequalities follow from (16) and (18), since $\Psi_r(S \cup N) > \Psi_r(S)$. Thus, all that can be concluded in general is that $\max\{d(r), e(r)\} \leqslant d_S(r) + e_N(r)$, equality holding for disjoint S and N.

The difficulty with the nondisjoint model is that the optimal value or r cannot be obtained from minimizing $\mathrm{E}[e(r)]$ as given in (15). Employing the current notation, in the disjoint model (15) is rewritten as

$$\mathrm{E}[e(r)] = \mathrm{E}[d(r)] = \mathrm{E}[d_S(r)] + \mathrm{E}[d_N(r)], \tag{20}$$

whereas in the nondisjoint model there is no reduction to $d_S(r)$ and $d_N(r)$ and we are stuck with

$$\mathrm{E}[e(r)] = \mathrm{E}[e_S(r)] + \mathrm{E}[e_N(r)]. \tag{21}$$

Equation (20) provides estimation from the individual pattern spectra, whereas (21) does not. A fundamental question arises: Can we predict r from (20) and get an error comparable to that resulting from minimization of (21)?

One way of approaching the problem is to consider the difference between the true value of $\mathrm{E}[e(r)]$ given by (21) and that given by (20) when using (20) as an approximation in the nondisjoint setting. Suppose we can find bounds K_0 and K_1 so that the difference $\mathrm{E}[e(r)] - \mathrm{E}[d(r)]$ satisfies

$$K_0 \leqslant \mathrm{E}[e(r)] - \mathrm{E}[d(r)] \leqslant K_1. \tag{22}$$

If $r^{\wedge\wedge}$ is found by minimizing $\mathrm{E}[d(r)]$,which is expressed in terms of the pattern spectra, whereas $r^{\wedge}$ is the true optimal solution for $\mathrm{E}[e(r)]$, then two inequalities can be deduced from (22):

$$\begin{aligned} \mathrm{E}[d(r^{\wedge\wedge})] + K_0 &\leqslant \mathrm{E}[e(r^{\wedge})] \leqslant \mathrm{E}[e(r^{\wedge\wedge})] \\ &\leqslant \mathrm{E}[d(r^{\wedge\wedge})] + K_1, \\ \mathrm{E}[e(r^{\wedge})] - K_1 &\leqslant \mathrm{E}[d(r^{\wedge\wedge})] \leqslant \mathrm{E}[e(r^{\wedge})] - K_0. \end{aligned} \tag{23}$$

A consequence of the first inequality is that selection of r by means of $\mathrm{E}[d(r)]$ minimization will yield a τ-opening whose error lies between the minimal possible error and $\mathrm{E}[d(r^{\wedge\wedge})] + K_1$. Combining this observation with the second inequality yields

$$\mathrm{E}[e(r^{\wedge})] \leqslant \mathrm{E}[e(r^{\wedge\wedge})] \leqslant \mathrm{E}[e(r^{\wedge})] + K_1 - K_0. \tag{24}$$

Consequently, $K_1 - K_0$ provides a bound on the error difference resulting from finding r directly

from the signal and noise pattern spectra when the signal and noise are not disjoint. In general, the difference problem is very difficult; we will consider a special case.

7. Nondisjoint signal and noise: a random-grain model

To get an idea of the types of error differences that occur, consider an image comprised of two intersecting circular grains S and N, where S is the signal, N is the noise, s is the radius of S, n is the radius of N, and $n<s$. There are three subcases:

$$\begin{aligned}
&\text{(a)}\ r<n<s \Rightarrow e_S(r)=0=d_S(r),\\
&\qquad\qquad e_N(r)=A[N-S]<A[N]=d_N(r),\\
&\text{(b)}\ n<r<s \Rightarrow e_S(r)=0=d_S(r),\\
&\qquad\qquad e_N(r)=A[Q_r]\geq 0=d_N(r),\\
&\text{(c)}\ n<s<r \Rightarrow e_S(r)=A[S]=d_S(r),\\
&\qquad\qquad e_N(r)=0=d_N(r),
\end{aligned} \tag{25}$$

where Q_r is the region depicted in Fig. 1. Two points should be recognized: (1) in case (b), $e_N(r)=A[Q_r]=0$ if and only if $N<S$; (2) in all three subcases (of this example) $e_S(r)=d_S(r)$. There exists a corresponding analysis if $s<n$ (which hopefully will happen with low probability):

$$\begin{aligned}
&\text{(a)}\ r<s<n \Rightarrow e_S(r)=0=d_S(r),\\
&\qquad\qquad e_N(r)=A[N-S]<A[N]=d_N(r),\\
&\text{(b)}\ s<r<n \Rightarrow e_S(r)=A[S-(N\cup W_r)]\\
&\qquad\qquad\qquad\qquad <A[S]=d_S(r),\\
&\qquad\qquad e_N(r)=A[N-S]<A[N]=d_N(r),\\
&\text{(c)}\ s<n<r \Rightarrow e_S(r)=A[S]=d_S(r),\\
&\qquad\qquad e_N(r)=0=d_N(r),
\end{aligned} \tag{26}$$

where W_r is defined analogously to Q_r.

Proceeding, suppose S and N are given by (6) and that $S\cup N$ is given by (7) with S and N not necessarily disjoint. First suppose S and N consist of single grains. Assuming E[N] is sufficiently less than E[S], it is most likely that subcase (b) of (25) will hold for an r value that is near optimal. For case (b) there is a full restoration if $N<S$. Therefore, we concentrate on case (b) when N is not a subset of S, in which case $n<r<s$ and the center of the grain N is within n of the boundary of S. Given the location of the noise-grain center, it is possible to find $e_N(r)$ exactly, but the expression is complicated and does not lead to a closed-form solution. However, there are simple bounds on $e_N(r)$:

$$0<e_N(r)<\pi n^2/2. \tag{27}$$

Tighter bounds are possible if further constraints are placed on the radii distibutions; however, given the current assumptions, the bounds are tight. Indeed,

$$\lim_{\substack{s\to\infty\\ r\to n}} e_N(r)=\pi n^2/2, \qquad \lim_{\substack{s\to\infty\\ r\to\infty}} e_N(r)=0. \tag{28}$$

Let us return to the case of a and b grains, as in (7). For the present, we make the assumption that the maximum noise-grain radius is smaller than the minimum signal-grain radius. While this assumption is overly strict, it does allow a straightforward analysis because, for optimal r, case (b) of (25) holds for all signal-noise pairs. Moreover, even if we consider a single signal grain in the presence of

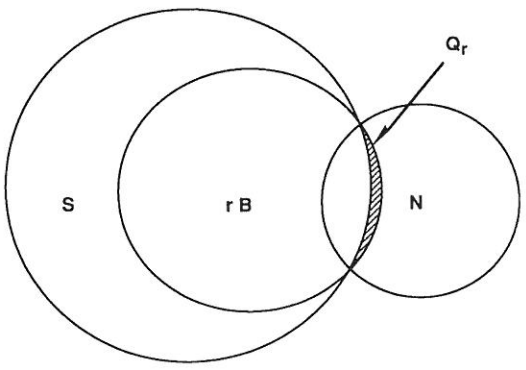

Fig. 1. Error Q_r.

many noise grains, it is still not possible to have $e_S(r) < d_S(r)$, so we can proceed under the assumption that $e_S(r) = d_S(r)$. Later, we consider the effect of weakening the assumption.

Consider a single noise grain $nB+z$ and let the signal grains be denoted as in (6). Let $D(r) = e(r) - d(r)$, which under the governing assumption is simply $e_N(r)$. Treating $D(r)$ as a random variable, we denote it by $\boldsymbol{D}$. We would like to find a bound on $\mathrm{E}[\boldsymbol{D}]$. $\boldsymbol{D}=0$ unless the center of $nB+z$ falls within n of a signal-grain boundary. If A denotes the entire image-frame area and we assume the grain is thrown randomly upon the image, then the probability that $\boldsymbol{D}\neq 0$ is

$$P(\boldsymbol{D}\neq 0) = A^{-1}\left(\sum_{i=1}^{a}\pi(s_i+n)^2 - \sum_{i=1}^{a}\pi(s_i-n)^2\right)$$
$$= 4\pi n A^{-1}\sum_{i=1}^{a} s_i = 4\pi a n \bar{s}, \tag{29}$$

where $\bar{s}$ is the mean of the s_i. Now define the random variable $\boldsymbol{Y}$ by $\boldsymbol{Y}=1$ if $\boldsymbol{D}\neq 0$ and $\boldsymbol{Y}=0$ if $\boldsymbol{D}=0$. Then, using a well-known result concerning conditional expectation, we obtain

$$\mathrm{E}[\boldsymbol{D}] = \mathrm{E}[\mathrm{E}[\boldsymbol{D}|\boldsymbol{Y}, \boldsymbol{N}]]$$
$$= \int_{-\infty}^{\infty}\int_{-\infty}^{\infty} \mathrm{E}[\boldsymbol{D}|\boldsymbol{Y}=y, \boldsymbol{N}=n] f_{Y,N}(y,n)\,\mathrm{d}y\,\mathrm{d}n$$
$$= \int_{-\infty}^{\infty}\int_{-\infty}^{\infty} \mathrm{E}[\boldsymbol{D}|\boldsymbol{Y}=y, \boldsymbol{N}=n] \times f_{Y|N}(y|n) f_N(n)\,\mathrm{d}y\,\mathrm{d}n$$
$$= 4\pi a\bar{s}A^{-1}\int_{-\infty}^{\infty} \mathrm{E}[\boldsymbol{D}|\boldsymbol{Y}=1, \boldsymbol{N}=n] n f_N(n)\,\mathrm{d}n$$
$$< 2\pi^2 a\bar{s}A^{-1}\int_{-\infty}^{\infty} n^3 f_N(n)\,\mathrm{d}n$$
$$= 2\pi^2 a\bar{s}\,\mathrm{E}[\boldsymbol{N}^3]A^{-1}. \tag{30}$$

Since there are b noise grains, we multiply the latter bound by b, and, recognizing that the computation was done for a single realization, we take the expected value over s to obtain

$$0 \leqslant \mathrm{E}[e(r) - d(r)] < 2\pi^2 ab\,\mathrm{E}[\boldsymbol{S}]\,\mathrm{E}[\boldsymbol{N}^3]A^{-1}, \tag{31}$$

nonnegativity following from $\boldsymbol{D}\geqslant 0$ under the assumption of signal–noise distributional separation. Relative to (22), the bounds are given by $K_0 = 0$ and $K_1 = 2\pi^2 ab\,\mathrm{E}[\boldsymbol{S}]\,\mathrm{E}[\boldsymbol{N}^3]A^{-1}$, and in terms of (24),

$$\mathrm{E}[e(r\hat{})] \leqslant \mathrm{E}[e(r\hat{}\hat{})]$$
$$< \mathrm{E}[e(r\hat{})] + 2\pi^2 ab\,\mathrm{E}[\boldsymbol{S}]\,\mathrm{E}[\boldsymbol{N}^3]A^{-1}. \tag{32}$$

If we select $r\hat{}\hat{}$ (from the signal and noise pattern spectra) to minimize $\mathrm{E}[d(r)]$, we can employ $O(S\cup N, r\hat{}\hat{}B)$ as a suboptimal filter and be assured that its performance is not worse than the bound given by (32).

Let us now consider the effect of dropping the restriction that the maximum value of the n_i is less than the minimum value of the s_i. The problem of obtaining bounds K_0 and K_1 becomes substantially more difficult. No longer can we be assured that $D(r) = e_N(r)$ or that inequality (27) holds, the latter ensuring $\mathrm{E}[\boldsymbol{D}|\boldsymbol{Y}=1, \boldsymbol{N}=n] < \pi n^2/2$ in (27). We must more closely consider the preceding conditional expectation. We proceed approximately, denoting the conditional expectation by Ω and considering, as in (27), a single noise grain being tossed upon S, as given in (6). Write the difference as

$$D(r) = e_S(r) - d_S(r) + e_N(r) - d_N(r)$$
$$= D_S(r) + D_N(r). \tag{33}$$

According to (25) and (26), $D_S(r) = 0$ unless there exist s_i such that $s_i < r < n$, which is condition (b) of (26). If there exist such i, say $I \leqslant i < I'$, then

$$D_S(r) = \sum_{i=I}^{I'} A[s_iB + x_i - (N\cup W(i)_r)] - A[s_iB + x_i]$$
$$= -\sum_{i=I}^{I'} A[N\cup W(i)_r]. \tag{34}$$

The negative expression for $D_S(r)$ shows us that it is possible for Ω to be negative, so that K_0 may not be 0 in (31). As for D_N it is negative for three situations, (a) of (25), (a) of (26) and (b) of (26).

In each case, a computation analogous to (34) applies. D_N is only positive in case (b) of (25), and here the previous analysis leading to (27) applies.

The error bound of (31) results from integrating Ω against $nf_N(n)$ and then taking the expectation against $\bar{S}$. Since dropping the original distributional restriction can never increase Ω, the original upper bound K_1 still holds, albeit a bit less tightly. However, because of the possibilities for Ω being negative, we can no longer claim a lower bound $K_0 = 0$. Yet, if $E[N]$ is sufficiently less than $E[S]$, then, for r close to optimal, the probabilities of the events leading to negative Ω are relatively small, so that employing $K_0 = 0$ is a reasonable approximation. Consequently, we can still use (31), recognizing the lower bound to be approximate and the upper bound to be loose. Of course, if one has reason to distrust the lower bound approximation on distributional grounds, then one can still apply the upper bound.

We consider an example for normal S and normal N. First, since N is normal, $E[N^3] = 5E[N]^3 + 3E[N]\,\mathrm{Var}[N]$. Suppose the image is 200×200, the signal has $a = 25$ grains, the noise has $b = 100$ grains, the signal radii possess the normal distribution Normal(3, 0.5), and the noise radii are normally distributed with Normal(0.5, 0.1). Then $K_1 = 2.29$. Recognizing the strong distributional difference, we apply (31) and obtain

$$E[e(r\hat{})] \leqslant E[e(r\hat{}\hat{})] \leqslant E[e(r\hat{})] + 2.29. \quad (35)$$

Considering that the total signal area is in the vicinity of 700 and the total noise area is in the vicinity of 80, a loss of performance of 2.29 is not great when the advantage is estimation directly from the individual pattern spectra.

8. Simulations

To demonstate optimal parameter selection, we have performed a number of simulations, a main intent being to compare $r\hat{}$ and $r\hat{}\hat{}$ in the cases where signal and noise overlap. The results of these simulations are summarized in the tables. In each table, all parameters employed to generate the signal image are listed in column Signal. The signal image may contain balls (Table 1), vertical lines (Table 2), horizontal lines (Table 3) or both horizontal and vertical lines (Table 4). The patterns used to generate the signal image, called *signal patterns*, are uniformly distributed on a 256×256 image. The length of the signal pattern is normally distributed with mean and variance listed in column Signal; however, the width may be fixed (Tables 1 and 2) or variable (Tables 3 and 4). In the latter case the length-to-width ratio of the structuring element must be fixed so that it only depends on a signal parameter. In Tables 3 and 4, this ratio is (mean signal length)/(mean signal width), these being 3.75 and 2.5, respectively. The number of signal patterns in the signal image is determined by the signal-to-noise ratio and the total number of noise patterns. For the noise images, all parameters are listed in the two columns labeled Noise. The noise image may contain balls, vertical lines or horizontal lines. The patterns (*noise patterns*) used to generate the noise image are also uniformly distributed on 256×256 images. The length of each noise pattern is normally distributed with mean and variance listed in the second Noise column; however, the width of the noise may be fixed (Tables 1 and 2) or normally distributed (Tables 3 and 4) with mean and variance listed in the first Noise column. The number of the various noise patterns being employed are listed in the first Noise column. We have discussed optimal estimation for both the nonoverlapping case and the overlapping case. Since we have demonstrated that $r\hat{} = r\hat{}\hat{}$ in the nonoverlapping case, it is not considered in the tables.

For each table, the signal process is the same throughout, but the noise-process is different in each row. Each row corresponds to a simulation that consists of a signal image, a noise image, a computation of $r\hat{}$ and $E[e(r\hat{})]$ by means of the actual symmetric-difference error, and a computation of $r\hat{}\hat{}$ and $E[e(r\hat{}\hat{})]$ by means of the signal and noise pattern spectra. Of particular note is the closeness of $r\hat{}$ and $r\hat{}\hat{}$ throughout. Only in three

Table 1
Signal image (balls) versus noise images (different patterns)

Signal	Noise	Noise var = 4	$e(r) = (S\hat{} - S) \cup (S - S\hat{})$		$d(r) = A[N](1 - \Phi_N(r)) + A[S]\Phi_S(r)$	
			$r\hat{}$	min E[$e(r\hat{})$]	$r\hat{}\hat{}$	min E[$d(r\hat{}\hat{})$]
Ball	Ball	mean: 4	9	85	9	64
SNR: 2.0	# = 50	mean: 8	12	5146	13	7188
Length:	Width:	mean: 9	13	5108	12	6887
Mean: 15	Fixed: 1	mean: 10	13	6113	13	9668
Var: 9		mean: 11	12	7062	14	12001
		mean: 12	13	8030	14	14959
Width:	H-Line	mean: 8	4	315	4	69
Fixed: 1	# = 1000	mean: 9	4	347	4	70
	Width:	mean: 10	4	415	4	62
	Fixed: 1	mean: 11	4	442	4	69
		mean: 12	6	506	4	78
Overlap	V-Line	mean: 8	4	317	3	67
	# = 1000	mean: 9	4	355	4	65
	Width:	mean: 10	4	398	4	60
	Fixed: 1	mean: 11	4	498	4	82
		mean: 12	6	473	4	74

Table 2
Signal image (vertical lines) with noise images (different patterns)

Signal	Noise	Noise var = 4	$e(r) = (S\hat{} - S) \cup (S - S\hat{})$		$d(r) = A[N](1 - \Phi_N(r)) + A[S]\Phi_S(r)$	
			$r\hat{}$	min E[$e(r\hat{})$]	$r\hat{}\hat{}$	min E[$d(r\hat{}\hat{})$]
V-Line	Ball	mean: 4	8	204	8	151
SNR: 2.0	# = 50	mean: 8	11	5525	12	6783
Length:	Width:	mean: 9	12	7082	13	8995
Mean: 15	Fixed: 1	mean: 10	11	7736	13	10930
Var: 9		mean: 11	12	8847	13	13713
		mean: 12	12	8845	13	14924
Width:	H-Line	mean: 8	2	2	2	1
Fixed: 1	# = 1000	mean: 9	2	2	2	1
	Width:	mean: 10	2	2	2	1
	Fixed: 1	mean: 11	2	3	2	1
		mean: 12	2	4	2	2
Overlap	V-Line	mean: 8	11	402	11	403
	# = 1000	mean: 9	12	507	12	501
	Width:	mean: 10	12	571	12	502
	Fixed: 1	mean: 11	13	751	13	761
		mean: 12	14	896	13	909

instances do they differ by more than 1, and in those cases the noise is close to the signal, so that we cannot expect very good filtering in any event.

The optimality estimates $r\hat{}$ and $r\hat{}\hat{}$ were obtained by using ten simulations of each image-noise pair. For $r\hat{}$, using the ten simulations, $e(r)$ was computed as a function of r for each [by means of (3)], and for each r the mean of the ten $e(r)$ values was computed, thereby giving an estimate for E[$e(r)$], the mean of random function $e(r)$. The value of r that minimized this estimate is taken as $r\hat{}$. As for $r\hat{}\hat{}$, the individual pattern spectra were

Table 3
Signal image (horizontal lines); noise image (horizontal lines, different lengths)

Signal	Noise	Noise length	Structuring element length to width ratio	$e(r)=(S\hat{}-S)\cup(S-S\hat{})$ $r\hat{}$	min E[$e(r\hat{})$]	$d(r)=A[N](1-\Phi_N(r))+A[S]\Phi_S(r)$ $r\hat{}\hat{}$	min E[$d(r\hat{}\hat{})$]	Optimal filter
H-Line	H-Line	mean: 4	3.75	9	309	9	309	$L=9$, $W=2$
SNR: 2.0		mean: 6	3.75	11	974	11	901	$L=11$, $W=2$
Length:	Length:	mean: 8	3.75	11	2086	12	2142	$L=12$, $W=2$
Mean: 15		mean: 10	3.75	12	2823	12	2972	$L=12$, $W=3$
Var: 9	Var: 4	mean: 12	3.75	12	3947	13	4222	$L=12$, $W=3$
Width	Width:							
Mean: 4	Mean: 2							
Var: 4	Var: 1							
Element:	Elements: 200							
Overlap								

Table 4
Signal image (horizontal lines and vertical lines); noise image (horizontal lines only)

Signal	Noise	Noise length	Structuring element length to width ratio	$e(r)=(S\hat{}-S)\cup(S-S\hat{})$ $r\hat{}$	min E[$e(r\hat{})$]	$d(r)=A[N](1-\Phi_N(r))+A[S]\Phi_S(r)$ $r\hat{}\hat{}$	min E[$d(r\hat{}\hat{})$]	Optimal filter
H&V-Line	H-Line	mean: 4	2.5	9	336	9	314	$L=9$, $W=3$
SNR: 2.0		mean: 6	2.5	9	793	9	748	$L=10$, $W=3$
Length:	Length:	mean: 8	2.5	10	1358	10	1287	$L=10$, $W=4$
Mean: 15		mean: 10	2.5	10	1868	11	1814	$L=11$, $W=4$
Var: 9	Var: 4	mean: 12	2.5	10	2527	10	2610	$L=10$, $W=4$
Width	Width:							
Mean: 6	Mean: 2							
Var: 4	Var: 1							
Element:	Elements: 200							
Overlap								

taken in each case, $d(r)$ was computed according to (15) for various values of r, and these were averaged to obtain an estimate of the random-function mean E[$d(r)$]. The value of r that minimized this estimate was taken as the optimal value $r\hat{}\hat{}$, which, as has been demonstrated, would be optimal were the signal and noise processes disjoint. It should be recognized that in the nonoverlapping-simulation estimate $r\hat{}\hat{}$; we not only do not require the signal and noise to be disjoint, we also do not require the signal or the noise to be comprised of disjoint patterns, which is a modeling assumption for the pattern-spectrum method yielding $r\hat{}\hat{}$.

We consider some specific results. From left to right in the top row of Fig. 2(a) we see a ball-generated signal image S with radius possessing mean 15 and variance 9, a ball-generated noise image N with radius possessing mean 4 and variance 4, nonoverlapping $S\cup N$, and the optimally filtered signal using $r=9$. The second row of the figure, which corresponds to the first row of Table 1, is similar except $S\cup N$ is not a disjoint union. Figure 3(a) shows four of the ten $e(r)$ realizations together with the mean estimate E[$e(r)$] for the overlapping process, $r\hat{}$ having been selected by finding the low point on the mean curve. Figure

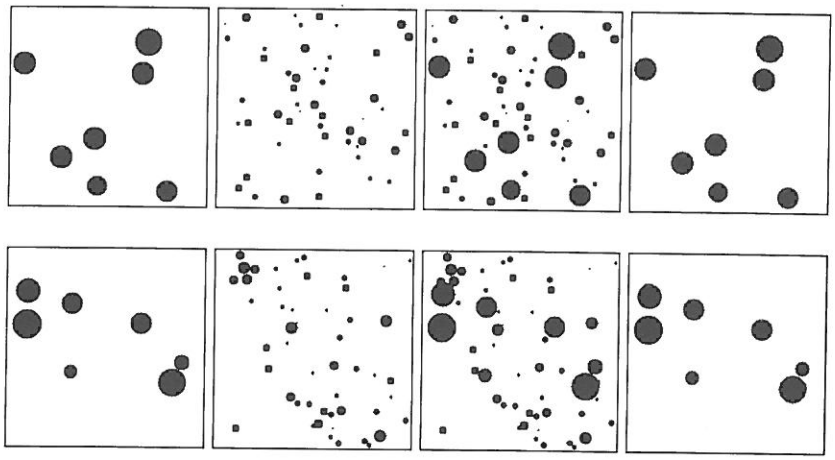

Fig. 2. Random ball image with small-ball noise.

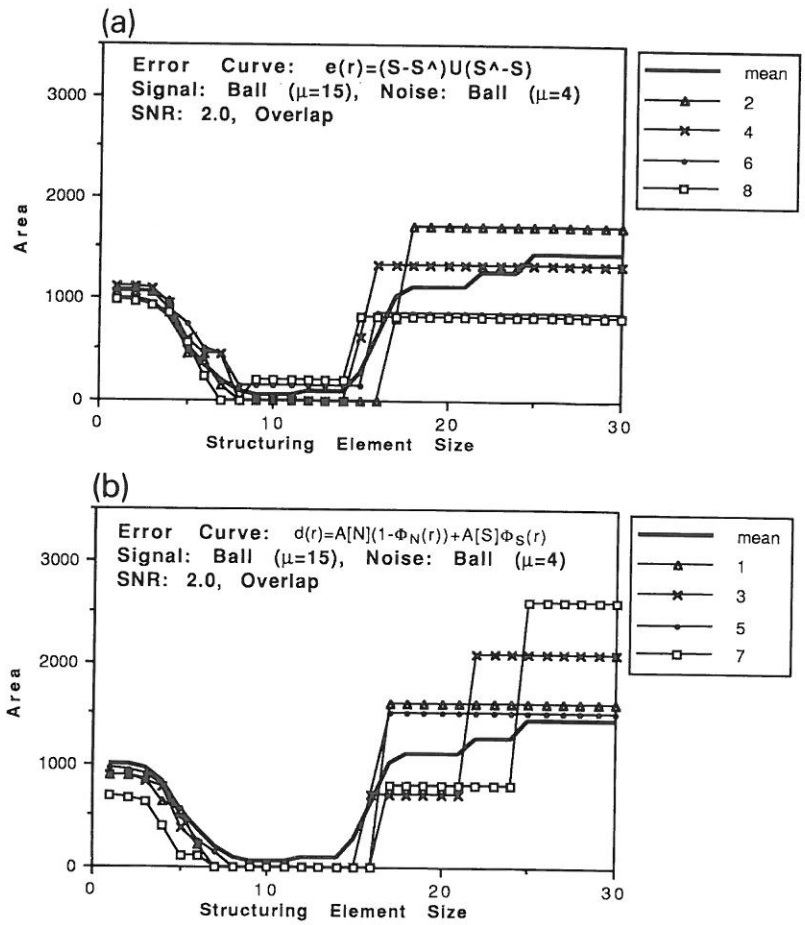

Fig. 3. Error curves corresponding to Fig. 2.

3(b) shows four of the ten $d(r)$ realizations together with the mean estimate $E[d(r)]$, $r^{\wedge\wedge}$ having been selected by finding the low point on the curve.

The image and noise realizations of Fig. 4 are analogous to those of Fig. 2, except here we employed noise with radius mean 8 and radius variance 4, the signal process being the same as in Fig. 2. These processes correspond to the second row of Table 1. $E[e(r)]$ minimization yields $r^{\wedge} = 12$ and $E[d(r)]$ minimization yields $r^{\wedge\wedge} = 13$. Both realizations of Fig. 4 have been filtered using $r^{\wedge} = 12$. Note that the optimal filter has not performed as well in Fig. 4 as in Fig. 2. This should not be surprising since in Fig. 4 the noise process is much more similar to the signal process.

Further simulations are given in subsequent figures: Fig. 5 corresponds to the second row of Table 2, Fig. 6 to the first row of Table 3, Fig. 7 to the first row of Table 4 and Fig. 8 to the third row of Table 4.

From a strictly mathematical perspective, our intent in providing the foregoing simulations has been to demonstrate experimentally the relationship between $r^{\wedge}$ and $r^{\wedge\wedge}$; however, reference to the simulations can also provide an intuitive, real-world appreciation of the estimation methodology. From the perspective of the random-grain model, $(S \cup N)$-realization grains not containing at least one τ-opening primitive are removed, and our purpose has been to do this optimally. The geometric character of the optimization is best illustrated by (11), in which it is seen that error results from erroneously removing small signal components and erroneously leaving large noise components, and that minimization of $E[e(r)]$ is the necessary mathematical requirement for choosing an optimal filter. This particle interpretation is best illustrated in the simulations of Figs. 2 and 4.

A variation of the particle interpretation can be achieved by considering Figs. 7 and 8. According to the procedure adopted by Loce and Dougherty [3, 9–11] for morphological restoration of print images via the Matheron representation theorem [15], an optimal (or suboptimal) morphological filter is derived via a random-process model and is then applied to a corrupted print image to accomplish restoration; in fact, the printed-character image will not strictly satisfy the model requirements, but good practical restoration is still achieved. As is illustrated in Figs. 7 and 8, optimal τ-opening restoration can be applied to restore an image composed of varied horizontal and vertical strokes, the optimality procedure determining which size strokes are to be eliminated. Viewing these strokes as character components permits τ-opening optimization to be applied to print images corrupted by background pepper components.

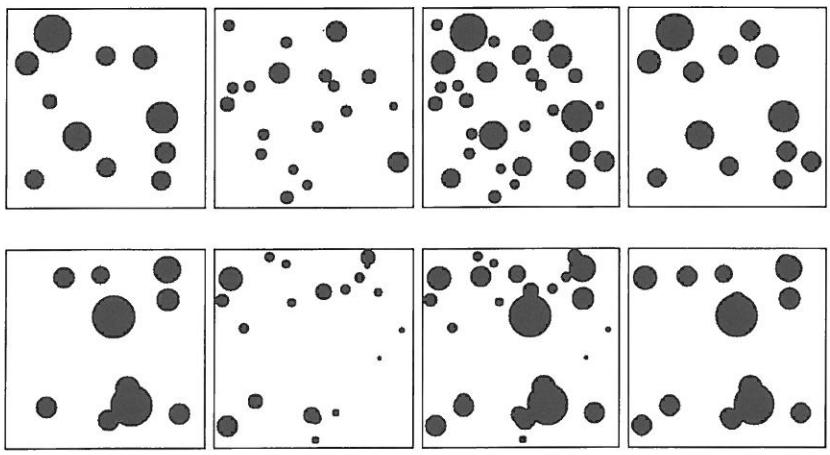

Fig. 4. Random ball image with large-ball noise.

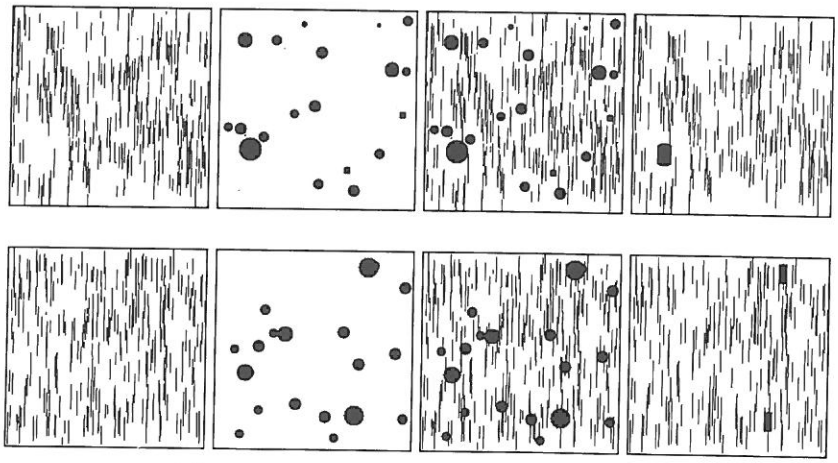

Fig. 5. Random vertical-line image with ball noise.

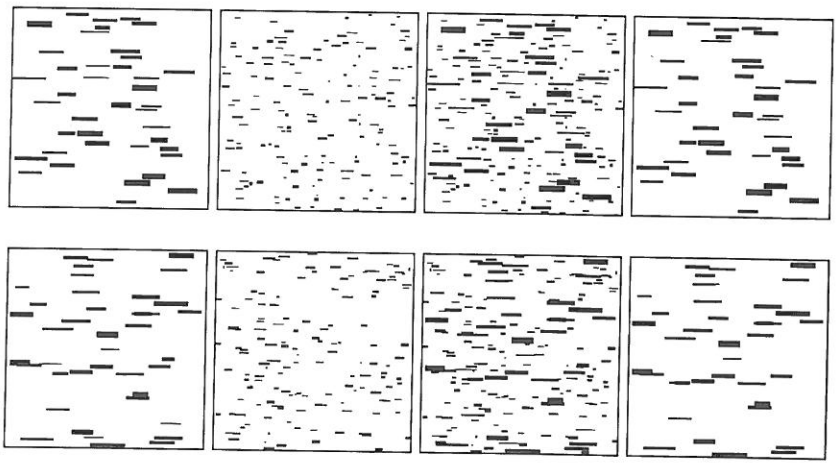

Fig. 6. Random horizontal-line with horizontal-line noise.

Still another interpretation can be given to the optimization procedure by considering Fig. 5: the image consists of objects of interest together with 'clutter', objects not of interest, and the goal is to remove the clutter so as to reveal the objects of interest (perhaps for identification purposes). In Fig. 5 the vertical lines are of interest and the balls are clutter. Optimization involves determination of a best filter to eliminate the clutter.

9. Conclusion

Owing to the close relationship between granulometries and opening, in certain random-grain models it is possible to find statistically optimal τ-openings for the union noise model by considering granulometric size distributions for both signal and noise. Optimization is facilitated by decomposition of the symmetric-difference error into a sum of signal and noise errors. Full optimization occurs for disjoint signal and noise because signal and noise errors can be expressed in terms of signal and noise pattern spectra. In the nondisjoint model, the optimal filter parameter resulting from the pattern-spectra formula is only approximate because the signal and noise errors are not directly expressible in terms of the respective spectra. Nonetheless, as demonstrated both analytically for a particular

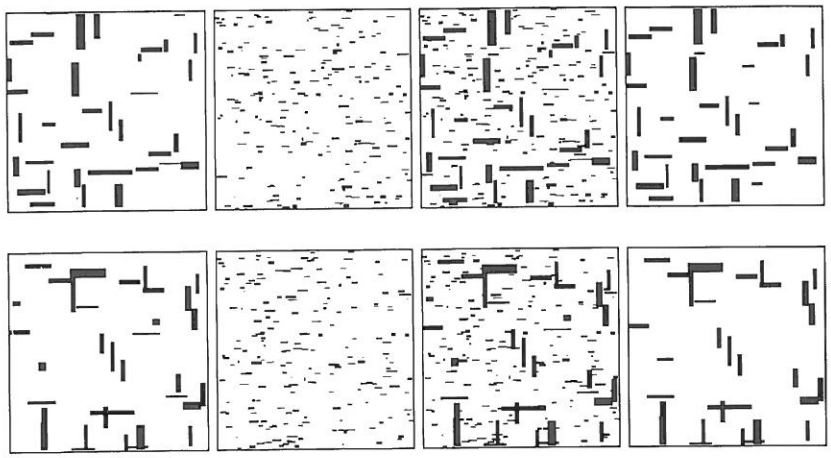

Fig. 7. Random vertical and horizontal line image with small-horizontal line noise.

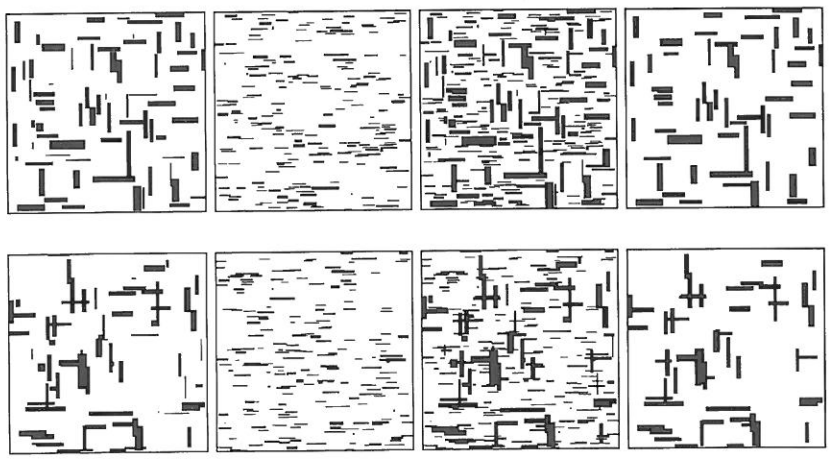

Fig. 8. Random vertical and horizontal line image with large-horizontal line noise.

image–noise model and experimentally for more complex models, approximating the optimal parameter in the nondisjoint case by employing pattern-spectra optimization yields opening parameters that are very close to optimal. Consequently, the method is quite robust relative to the disjointness hypothesis.

References

[1] C. Agerskov, U. Jacobi and P.H. Sloth, Parameter estimation of morphological algorithms for removing noise from binary images, *Internal Report*, Department of Electrical Engineering, University of Washington, Seattle, January 1990.

[2] E. Dougherty and C. Giardina, *Imaging Processing: Continuous to Discrete*, Prentice Hall, Englewood Cliffs, NJ, 1987.

[3] E.R. Dougherty, "Optimal mean-square N-observation digital morphological filters – Part 1: Optimal binary filters", *J. Comput. Vision Graph. Image Process. – Image Understanding*, Vol. 55, No. 1, January 1992.

[4] E. Dougherty and J. Pelz, "Pixel classification by morphologically derived texture features", *Proc SPIE*, Vol. 1199, Philadelphia, PA, 1989, pp. 440–449.

[5] E. Dougherty and J. Pelz, "Size distribution statistics for process control", *SPIE J. Opt. Engrg.*, Vol. 30, No. 4, April 1991, pp. 438–445.

[6] E.R. Dougherty, Y. Chen, S. Totterman and J. Hornak, "Detection of osteoporosis by morphological granulometries", *Proc. SPIE*, Vol. 1660, San Jose, 1992.

[7] E.R. Dougherty, J.B. Pelz, F. Sand and A. Lent, "Morphological image segmentation by local granulometic size distributions", *J. Electron. Imaging*, Vol. 1, No. 1, January 1992.

[8] C. Giardina and E. Dougherty, *Morphological Methods in Image and Signal Processing*, Prentice Hall, Englewood Cliffs, NJ, 1988.

[9] R.P. Loce and E.R. Dougherty, "Using structuring-element libraries to design suboptimal morphological filters", *Proc. SPIE*, Vol. 1568, San Diego, July 1991.

[10] R.P. Loce and E.R. Dougherty, "Document restoration by optimal morphological filters", *Proc. Internat. Conf. Imaging Science and Hardcopy*, Shanghai, May 1992.

[11] R.P. Loce and E.R. Dougherty, "Facilitation of optimal binary morphological filter design via structuring-element libraries and design constraints", *J. Opt. Engrg.*, Vol. 31, No. 5, May 1992, pp. 1008–1025.

[12] P. Maragos, "Pattern spectrum of images and morphological shape-size complexity", *IEEE Internat. Conf. Acoust. Speech Signal Process.*, Dallas, 1987, pp. 241–244.

[13] P. Maragos, "Morphological-based symbolic image modeling, multi-scale nonlinear smoothing, and pattern spectrum", *IEEE CVPR*, Ann Arbor, 1988, pp. 766–773.

[14] P. Maragos, "Pattern spectrum and multiscale representation", *IEEE Trans. Pattern Anal. Machine Intell.*, Vol. 11, No. 7, July 1989, pp. 701–716.

[15] G. Matheron, *Random Sets and Integral Geometry*, Wiley, New York, 1975.

[16] J. Newell and E.R. Dougherty, "Maximum-likelihood morphological granulometric classifiers", *Proc. SPIE*, Vol. 1657, San Jose, February 1992.

[17] D. Schonfeld, Optimal morphological representation and restoration of binary images: Theory and applications, Ph.D. Thesis, The Johns Hopkins University, Baltimore, 1990.

[18] D. Schonfeld and J. Goutsias, "Optimal morphological filters for pattern restoration", *Proc. SPIE*, Vol. 1199, November 1989, pp. 158–169.

[19] D. Schonfeld and J. Goutsias, "Optimal morphological pattern restoration from noisy binary images", *IEEE Trans. Pattern Anal. Machine Intell.*, Vol. 13, No. 1, January 1991, pp. 14–29.

[20] J. Serra, "Alternating sequential filters", in: J. Serra, ed., *Image Analysis and Mathematical Morphology*, Vol. 2, Academic Press, New York, 1988.

[21] J. Serra, *Image Analysis and Mathematical Morphology*, Academic Press, New York, 1982.